JOM, Vol. 67, No. 5, 2015
DOI: 10.1007/s11837-014-1269-4

Effect of Y Addition on the Mechanical Properties and Microstructure of Zn-Al Alloys

MINGYANG LI,[1] SHUJING LU,[1] FANG LONG,[3] MENG SHENG,[1] HAORAN GENG,[1,2,5,6] and WENDI LIU[4]

1.—School of Materials Science and Engineering, University of Jinan, Jinan 250022, P.R. China. 2.—Shandong Provincial Key Laboratory of Preparation and Measurement of Building Materials, University of Jinan, Jinan 250022, P.R. China. 3.—Shandong Binzhou Bohai Piston Co., Ltd., Binzhou 256602, P.R. China. 4.—School of Construction and Materials Engineering, College of Jining Technician, Jining 272000, P.R. China. 5.—e-mail: strong-422@163.com. 6.—e-mail: mse_genghr@ujn.edu.cn

This article will discuss the influence of the rare earth Y on the microstructure and mechanical properties of Zn-Al alloys (ZA27, ZA35, and ZA40), and it will provide reference to rare-earth microalloying through the cast ingot metallurgy process. The results also suggest that the microstructure can be refined and mechanical properties can be improved obviously when adding the right amount of Y, and its tensile strength and brinell hardness increased by 9.1% and 11.7% compared with the unmodified ZA27 alloys, respectively. Compared with non-Y addition, the alloys will form dispersed YZn_{12} phase, which can strongly pin dislocations and subgrain boundary, inhibiting further recrystallization. On this basis, the impacts of Y on the microstructure and mechanical properties of ZA27, ZA35, and ZA40 have been explored. After adding Y, the microstructures of as-cast Zn-Al alloys are refined at different degree. However, with the increase of Al content, the microstructure shows a certain coarsening and the segregation and shrinkage porosity occur. The most effective refining appears in ZA27-0.4%Y.

INTRODUCTION

Zinc-aluminium–based alloys have been widely used for several decades.[1,2] Zn-Al alloys could provide potential applications other than cast iron and brass because of their favorable comprehensive characteristics (super plasticity, low melting point, moderate strength, exceptional castability, easy machinability, and excellent wear resistance).[3–7] Al-Zn-Mg-Cu alloys (7xxx series Al alloys) have been also widely used in fields of machinery, aerospace, and automobile industries because of its remarkable combination of characteristics such as low density, high strength, and easy formability.[8,9] The microstructures of as-cast and homogenized alloys have been studied in detail and a lot of work has been done to investigate the strengthening mechanism.[10,11]

But with the rapid development of composite material and titanium alloy, high-strength aluminum alloy is facing unprecedented challenges. Improving the general properties of high-strength aluminum alloy has focused more and more on microalloying. It was well accepted that trace additions of rare-earth elements are of great importance to improve the mechanical properties and microstructure of aluminum alloys.[12] Y can effectively refine the branch crystal microstructure of as-cast alloy, inhibit the formation of bulky eutectic microstructure, and improve the elongation.[13,14] But due to the complexity of the Zn-Al alloy systems as well as the limit and difficulty of characterizing the effect of rare earth, no complete theories are available to guide the design of this type due to the lack of research on it. This article will discuss the effect of the rare earth Y in Zn-Al alloys (ZA27, ZA35, and ZA40), and it will provide reference to rare-earth microalloying through the cast ingot metallurgy process. The authors hope to improve the performance of Zn-Al alloys by adding Y.

EXPERIMENTAL SECTION

Al-Zn-Cu-Mg alloy was determined as the base alloy. The base alloy used in the experiment was

(Published online January 10, 2015)

prepared with commercial pure Al ingot (99.9 wt.%), pure Zn ingot (99.99 wt.%), Mg ingot (99.7 wt.%), Cu ingot (99.99 wt.%), Y ingot (99.9 wt.%), and Al-25%Cu and Al-10%Y master alloys in a medium-frequency induction furnace. The experiments were conducted in an electrical-resistance furnace in a pure argon atmosphere. The melt temperature was controlled by the thermocouple in the furnace and assisted by the handset laser thermometric indicator to ensure that the temperature discrepancy is controlled below ±5°C. All the samples were poured into the same permanent mold preheated to 200°C. The alloys were made by the conventional casting technique and melted in a graphite crucible using an electrical resistance furnace and kept at 640°C for 20 min.

The dimensions of the tensile strength test bars are shown in Fig. 1 using Chinese standard (GB/T 24196-2009). The value of ultimate tensile strengths was obtained. Tensile properties were evaluated by the WDW-100A (Enkay Enterprises, New Delhi, India) universal tester at a constant rate of 6 mm/min at room temperature. The metallographic specimens were all cut from the same position of the casting samples, then mechanically ground and polished using standard routines. Hardness was measured by an HBRV-187.5 (Wan Heng, Shanghai, China) sclerometer. Every sample was tested five times, and the average of them was obtained. The microstructure was analyzed and quantitatively analyzed using the M-4XC (Jiming Measuring Equipment, Shanghai, China) metallographic microscope with an image collection and analysis system. The analysis of rare-earth compounds was conducted using a QUANTAFEG250 (FEI, Portland, OR) scanning electron microscope (SEM) equipped with energy-dispersive x-ray spectroscopy (EDS). The Zn-Al alloys were identified by x-ray diffraction: The x-ray diffraction patterns were obtained using an XRD D8-advance diffractometer (Bruker, Karlsruhe, Germany) operated at 40 kV and 40 mA with Cu-Kα radiation and a wavelength of 0.15406 nm. The corrosion resistance of alloys was evaluated through electrochemical potentiodynamic polarization test (EC500, Gaoss Union, Wuhan, China) in an aqueous chloride solution (3.5%, NaCl).

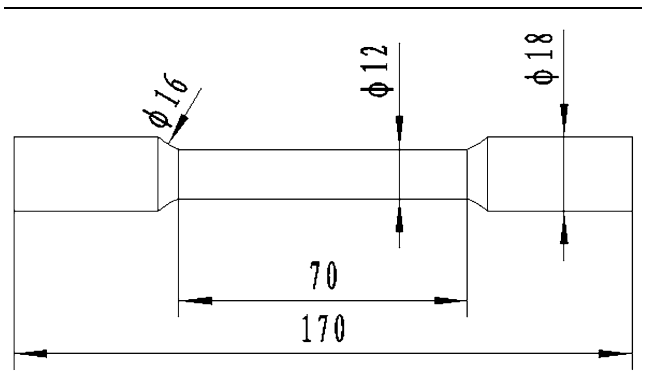

Fig. 1. Tensile specimen geometry and dimensions (unit: mm).

RESULTS AND DISCUSSION

Effect of Y Addition on the Mechanical Properties and Microstructure of ZA27 Alloys

The mechanical properties of the ZA27 alloys with Y contents are shown in Fig. 2. With the increase of Y contents, the mechanical properties show a downward trend after the first rise. It indicates that compared with non-Y addition alloy, adding Y can improve the tensile strength and hardness. When the alloy contains 0.4%Y, the ultimate tensile strength value is 434 MPa and the hardness is 128.2 HB. The improving amplitudes reach 9.1% and 11.7%, respectively. When adding 0.7%Y, the mechanical properties decline significantly.

The microstructures of the studied alloys are shown in Fig. 3. Coarsening as-cast grains, dendritic grains, and serious segregation can be obviously observed in Fig. 3a. The size of α-Al decreases and the morphology of the α-Al presents uniformly distribution (Fig. 3b) when only adding 0.1%Y. Adding rare earth could refine the grain and abate the dendritic grains. The most effective refining appears in Fig. 3c. With the addition of 0.4%Y, α-Al alters from dendrites to petaloid or equiaxial grains and become uniform. Compared with alloy adding 0.4%Y, simultaneously adding of 0.7%Y, the microstructure appears as dendritic grains, but it is still basically equiaxial crystal.

The SEM micrographs and XRD of ZA27-0.4%Y alloy are presented in Fig. 4. As shown in Fig. 4, in addition to α-Al phase and η-Zn phase in ZA27 alloy, ε phase exists in the form of $CuZn_5$. ε phase is a hard phase and is dispersively distributed along the α-Al grain boundaries, which can increase alloy hardness, strength, and wear resistance. Also there is a new phase YZn_{12} in the alloy. Based on the XRD, SEM and EDS, it is suggested that Y was dissolved in η-phase.

The corrosion resistance of ZA27 alloys was evaluated with an electrochemical potentiodynamic

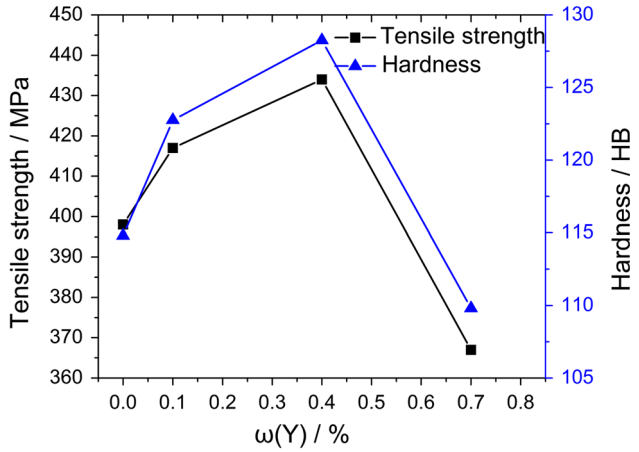

Fig. 2. Mechanical properties of ZA27 alloys with Y contents.

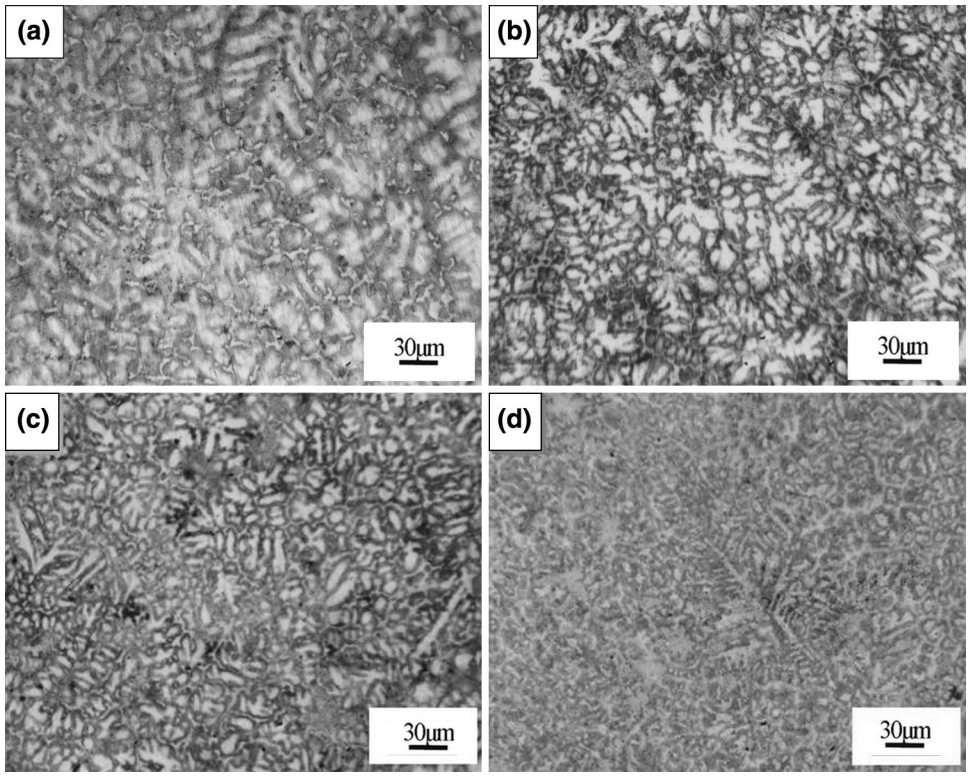

Fig. 3. Metallographic microstructure of ZA27 alloy: (a) 0%Y, (b) 0.1%Y, (c) 0.4%Y, and (d) 0.7%Y.

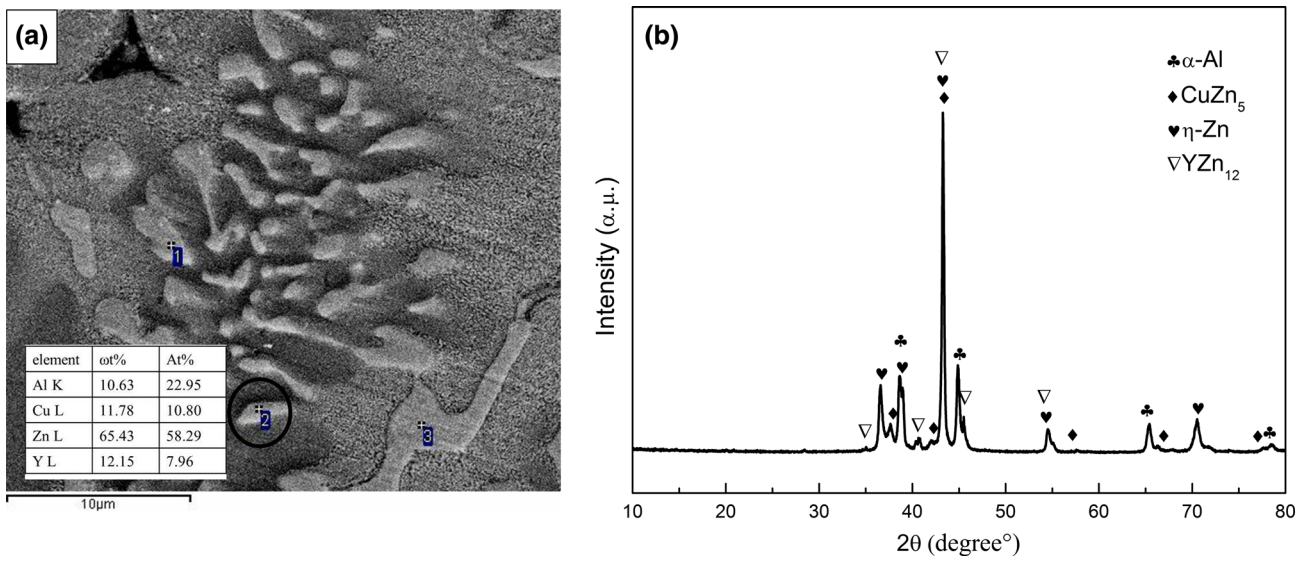

Fig. 4. The SEM micrographs and XRD of ZA27-0.4%Y alloy.

polarization test to reflect its organization and structure. Figure 5a displays the potentiodynamic polarization curves of ZA27 alloy with different Y contents in the aqueous chloride solution (3.5%, NaCl) with a potential between—1100 and 250 mV (SCE). As shown in Fig. 5a, with the increase of Y content, the potentiodynamic polarization curves show a trend to the right and then move to the left, indicating that their corrosion resistance improves with the increase of Y contents at a certain range.

Figure 5b is the fitting result of potentiodynamic polarization curves. The corrosion potential (E_{corr}) shows a decreasing trend after the first increase and the corrosion current density (i_{corr}) shows an increasing trend after the first decrease. The i_{corr} of alloy reduces greatly with addition of 0.4%Y, when

the amount of Y reaches 0.7% the i_{corr} rises, but it is still lower than the alloy without Y. The decrease of i_{corr} indicates that the corrosion resistance of alloy enhances, which corresponds to the trend shown in Fig. 5a. The experimental results show that Y can enhance the corrosion resistance of ZA27 alloy. When the alloy contains 0.4%Y, the ZA27 alloy has higher E_{corr} and lower i_{corr} than the other alloys, and its E_{corr} and i_{corr} increased by 16.1% and 15.6% compared with the unmodified ZA27 alloys, respectively. The results indicate that low Y content can improve the corrosion resistance of the ZA27 alloy, which is attributed to Y making the free corrosion potentials shift to positive and decreasing the corrosion current density. However, excessive Y content can deteriorate the corrosion resistance.

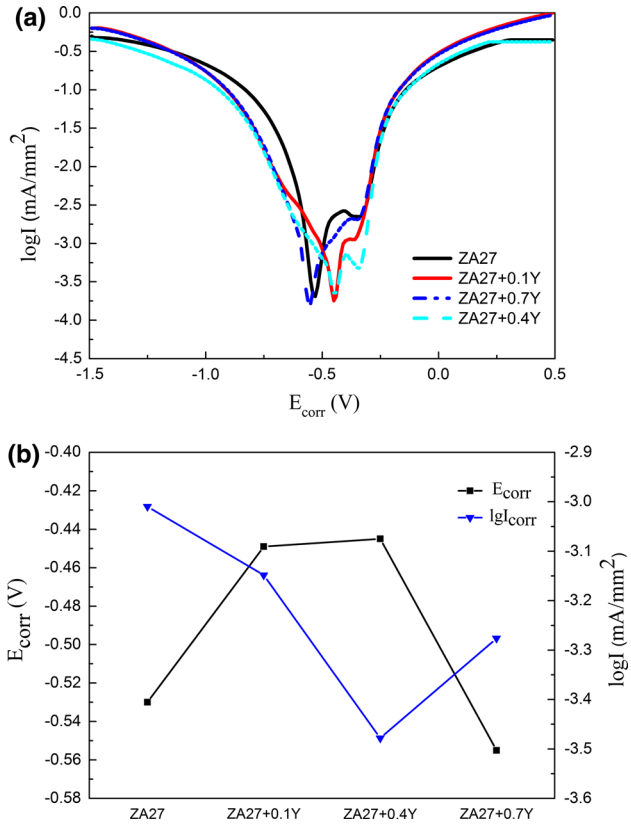

Fig. 5. Corrosion resistance of ZA27 with Y content: (a) potentiodynamic polarization curves and (b) potentiodynamic polarization curves fitting.

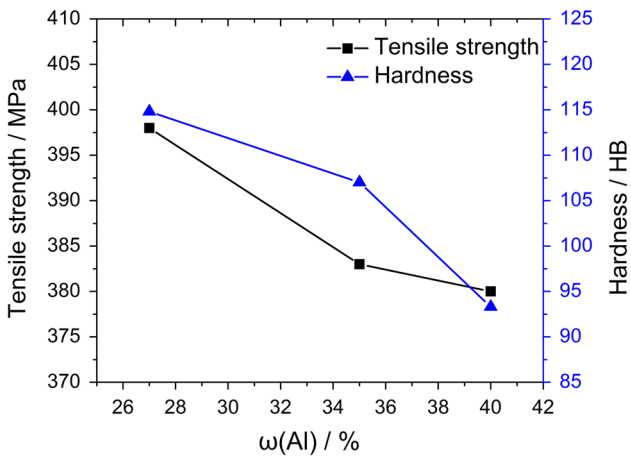

Fig. 6. Mechanical properties of ZA27, ZA35, and ZA40 alloys.

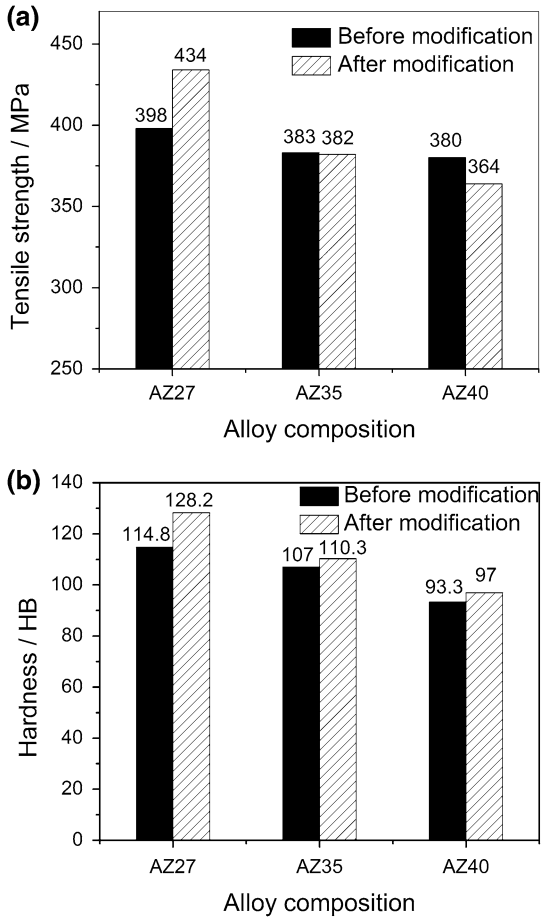

Fig. 7. Mechanical properties of ZA27, ZA35, and ZA40 alloys after adding 0.4%Y content.

tively. The results indicate that low Y content can improve the corrosion resistance of the ZA27 alloy, which is attributed to Y making the free corrosion potentials shift to positive and decreasing the corrosion current density. However, excessive Y content can deteriorate the corrosion resistance.

The research [15] shows that precipitates and presence of α-phase are the main reason of intergranular corrosion of Zn-Al alloys. In corrosion medium, α-Al and η-Zn phase dissolve as active anode and cathode, respectively. With the adding of Y, crystalline grains of α-Al are refined and the morphology of the α-Al presents uniform distribution, which can reduce the amount of the charge transfer between atoms in the alloy and the electrode potential between Zn and Al. The results show that intergranular corrosion can be inhibited and corrosion resistance be improved.

By adding Y, the crystalline grains of α-Al of the alloys in the as-cast structure are refined; this is related to the characteristic of Y in the process of solidification of the alloys. They can fill the vacancies on the surfaces when they dissolve in the alloys which can reduce the surface tension between two phases. Consequently, nucleation speed can in-

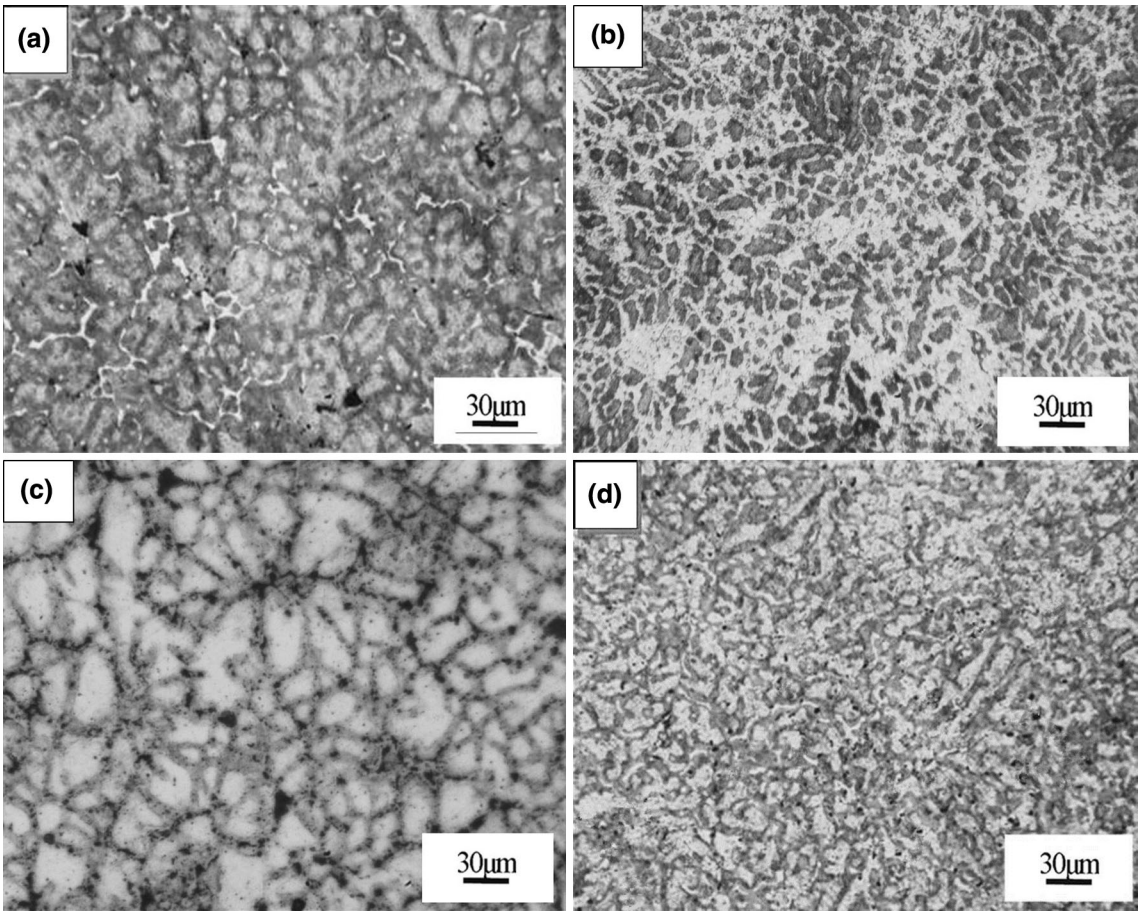

Fig. 8. Metallographic microstructure of ZA27, ZA35, and ZA40 alloys: (a) ZA35, (b) ZA35 + 0.4Y, (c) ZA40, and (d) ZA40 + 0.4Y.

crease. Meanwhile, active surface membranes form between grains and the liquid alloy, which block the growing of the grains and make the grains refined.[16] Grain refinement can be obtained. The chemical properties of Y elements are rather active and the electronegativity of Y is 1.22, smaller than Al (1.61) and Zn (1.65). They can form high-melting-point and high-hardness compounds, which are pushed to the dendrite or crystal grain boundaries. Thus, a discontinuous distribution is formed along the grain, which can reduce the grain boundary energy and the phase boundary energy and can improve the interface binding force. So they can effectively impede deformation and grain boundary migration.

The YZn_{12} particles that can strongly pin dislocations and grain boundary (as shown in Fig. 4) appear in the alloys. These particles block the movement of dislocations as well as sub-boundary and have a strong stabilization effect of the substructure of the deformation organization. It is suggested that Y displays slightly lower binding energy with vacancies than are exhibited by Mg and Zn,[17,18] which will automatically preferentially attach to vacancies and sequester them. Such a preferential binding of vacancies with Y results in a decrease in the number of vacancies available for the movement of Mg and Zn atoms. The refined crystalline grains of α-Al of the alloys in the as-cast structure and improved mechanical properties are directly related to the binding energy effect. However, with the increase of Y content, the hard and brittle second phase would grow and become segregated, which results in stress concentrations and reduced mechanical properties.

Effect of Y Addition on the Mechanical Properties and Microstructure of ZA35 and ZA40 Alloys

The mechanical properties of the ZA27, ZA35, and ZA40 alloys are shown in Fig. 6. With the increase of Al contents, the mechanical properties show a downward trend. This indicates that compared with low-Al alloy, high-Al alloy can reduce the tensile strength and hardness. When the Al content reaches 40%, the drop amplitudes of the ultimate tensile strength and the hardness values reach 4.5% and 18.7%, respectively. So the mechanical properties of ZA27 are the best. The hardness of η-Zn phase and $CuZn_5$ phase is higher than α-Al phase. With the increase of Al content, α-Al phase increases, which results in reduced mechanical properties.

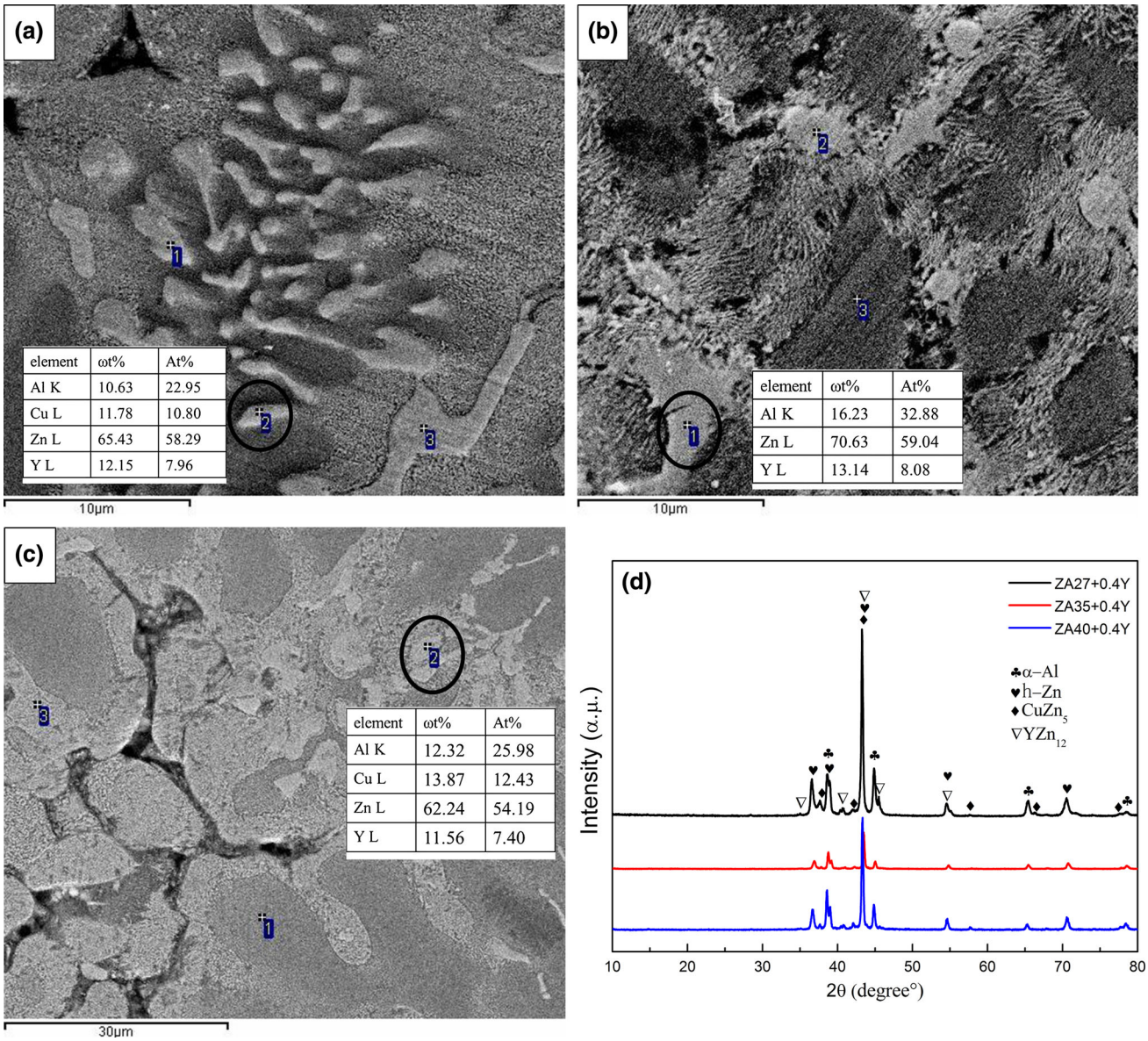

Fig. 9. The SEM micrographs and XRD of ZA27-0.4%Y, ZA35-0.4%Y, and ZA40-0.4%Y alloys: (a) ZA27 + 0.4Y, (b) ZA35 + 0.4Y, (c) ZA40 + 0.4Y, and (d) XRD.

Figure 7 shows the mechanical properties of ZA27, ZA35, and ZA40 alloys after adding 0.4%Y content. When the ZA27 alloy adds Y, the improving amplitudes of the ultimate tensile strength and the hardness values reach 9.1% and 11.7%, respectively. However, the tensile strength of ZA35 alloy is nearly unchanged and hardness increases by 3.1%; the tensile strength of ZA40 alloy decreases by 4.2% and hardness increases by 4.0%.

The microstructures of ZA35-0.4%Y and ZA40-0.4%Y alloy are presented in Fig. 8. As shown in Figs. 3a, and 8a and c, with the increase of Al content, α-Al phase increases and the microstructure shows coarsening and dendritic grains. After the addition of 0.4%Y, the microstructure of Zn-Al alloys have different levels of refinement, especially ZA27 alloy. Its slender dendritic grains change into regular petaloid or equiaxial grains (Fig. 3c). As shown in Fig. 8b and d, although crystalline grains are refined, the segregation and shrinkage porosity occur, which correspond to the microstructure shown in Fig. 9.

The SEM micrographs and XRD of ZA27-0.4%Y, ZA35-0.4%Y, and ZA40-0.4%Y alloys are presented in Fig. 9. As shown in Fig. 9a–c, Y content exists in η-Zn phase. The segregation and shrinkage porosity occur in Fig. 9b and c. As shown in Fig. 9d, there is YZn_{12} phase in Zn-Al alloys and the peaks of XRD of ZA27-0.4%Y are different from that of ZA35-0.4%Y and ZA40-0.4%Y, which indicated different crystallinity.

By adding Y, crystalline grains of ZA27, ZA35, after ZA40 alloys in the as-cast structure are refined in different degrees. The YZn_{12} particles can strongly pin dislocations and grain boundary, which can reduce the surface tension, make dendrite tip blunt, and refine the microstructure of the alloy effectively.

As shown in metallographic microstructures of ZA35 and ZA40 alloys, although crystalline grains are refined, the segregation and shrinkage porosity occur. According to the Zn-Al binary phase diagram, Zn-Al intermetallic compound might not be formed, the liquid phase dissolved limitlessly, and it has a wider solidification range. With the increase of Al content, the solidification range becomes wider; the result is that during solidification, α-Al phase dendrites precipitate first, the segregation and microscopic shrinkage porosity occur, and it has a larger impact on the mechanical properties of the Zn-Al alloys. The microscopic shrinkage porosity in the surface and subsurface can cause serious distortion in the stretching process. The irregular shrinkage under the effect of stress concentration can be directly a source of effective crack. And due to the low toughness of matrix, the formative cracks extend along the intergranular easily, which can form intergranular fracture. With the increase of Al content, the new YZn_{12} phases in the grain boundaries distribute unequally and segregate seriously. So high-Al alloy can reduce the tensile strength and hardness, compared with low-Al alloy.

CONCLUSION

From these results and discussions above, the major conclusions are summarized as follows:

(1). Compared with ZA27 alloy, the alloys with Y demonstrate improvements in strength, hardness, and corrosion resistance. When adding 0.4%Y elements, the tensile strength is 434 MPa, the hardness is 128.2 HB, and the improving amplitudes reach 9.1% and 11.7%, respectively. When the alloy contains 0.4%Y, the ZA27 alloy has higher E_{corr} and lower i_{corr} and its E_{corr} and i_{corr} increase by 16.1% and 15.6% compared with the unmodified ZA27 alloys, respectively.

(2). With the increase of Al contents, the mechanical properties of ZA27, ZA35, and ZA40 alloys show a downward trend. It indicates that compared with low-Al alloy, high-Al alloy can reduce the tensile strength and hardness. With the increase of Al content, α-Al phase increases, which results in reduced mechanical properties.

(3). After adding Y, the microstructures of as-cast Zn-Al alloys are refined at different degrees. However, with the increase of Al content, the microstructure shows coarsening and the segregation and shrinkage porosity occur. The most effective refining appears in ZA27-0.4%Y. Compared with non-Y addition, the alloys will form dispersed YZn_{12} phase, which can strongly pin dislocations and subgrain boundary, thereby inhibiting further recrystallization.

ACKNOWLEDGEMENT

The authors would like to acknowledge the National Natural Science Foundation of China (51271087, 51471076, and 51401085) for supporting this work.

REFERENCES

1. E. Gervais, H. Levert, and M. Bess, *Trans. Am. Foundrym. Soc.* 88, 183 (1980).
2. E.J. Kubel Jr, *Adv. Mater. Process* 132, 51 (1987).
3. S.H.J. Lo, S. Dionne, M. Sahoo, and H.M. Hawthorne, *J. Mater. Sci.* 27, 5681 (1992).
4. V.M. Lopez Hirata, M. Saucedo Muñoz, J.C. Rodriguez Hernandez, and Y.H. Zhu, *Mater. Sci. Eng. A* 247, 8 (1998).
5. Y.H. Zhu and J. Torres, *J. Mater. Process Tech.* 73, 25 (1998).
6. G. Pürçek, *J. Mater. Process Tech.* 169, 242 (2005).
7. P. Kumar, C. Xu, and T.G. Langdon, *Mater. Sci. Eng. A* 429, 324 (2006).
8. G. Dlubek, P. Lademann, H. Krause, S. Krause, and R. Unger, *Scripta Mater.* 39, 893 (1998).
9. A. Heinz, A. Haszler, C. Keidel, S. Moldenhauer, R. Benedictus, and W.S. Miller, *Mater. Sci. Eng., A* 280, 102 (2000).
10. X.Z. Li, V. Hansan, J. GjØnnes, and L.R. Wallenberg, *Acta Mater.* 47, 2651 (1999).
11. Y. Deng, Z.M. Yin, K. Zhao, J.Q. Duan, and Z.B. He, *Corros. Sci.* 65, 288 (2012).
12. S. Bai, Z.Y. Liu, Y.T. Li, Y.H. Hou, and X. Chen, *Mater. Sci. Eng. A* 527, 1806 (2010).
13. J.J. Yang, Z.R. Nie, T.N. Jin, H.Q. Ruan, and T.Y. Zuo, *Chin. J. Nonferrous Metall.* 14, 620 (2004).
14. X. Wang and Z. Nie, *Spec. Cast. Nonferrous Alloy* 29, 76 (2009).
15. P. Fan, L. Song, X.Z. Pang, and J.M. Zeng, *Spec. Cast. Nonferrous Alloy* 28, 401 (2008).
16. A.K. Chaubey, S. Mohapatra, B. Bhoi, J.L. Gumaste, B.K. Mishra, and P.S. Mukherjee, *Defect Diffus. Forum* 279, 97 (2008).
17. L.F. Mondolfo, *Aluminum Alloys: Structure and Properties* (London, UK: Butterworths, 1976).
18. V. Sudarshan, *Trans. Indian Inst. Metall.* 62, 209 (2009).